A&A 397, 667–674 (2003)
DOI: 10.1051/0004-6361:20021530

Astronomy & Astrophysics

An estimate of the time variation of the O/H radial gradient from planetary nebulae

W. J. Maciel, R. D. D. Costa, and M. M. M. Uchida

IAG/USP, 04301-904 São Paulo SP, Brazil
e-mail: maciel@astro.iag.usp.br;roberto@astro.iag.usp.br;monica@astro.iag.usp.br

Received 8 July 2002 / Accepted 18 October 2002

Abstract. Radial abundance gradients are a common feature of spiral galaxies, and in the case of the Galaxy both the magnitude of the gradients and their variations are among the most important constraints of chemical evolution models. Planetary nebulae (PN) are particularly interesting objects to study the gradients and their variations. Owing to their bright emission spectra, they can be observed even at large galactocentric distances, and the derived abundances are relatively accurate, with uncertainties of about 0.1 to 0.2 dex, particularly for the elements that are not synthesized in their progenitor stars. On the other hand, as the offspring of intermediate mass stars, with main sequence masses in the interval of 1 to 8 solar masses, they are representative of objects with a reasonable age span. In this paper, we present an estimate of the time variation of the O/H radial gradient in a sample containing over 200 nebulae with accurate abundances. Our results are consistent with a flattening of the O/H gradient roughly from −0.11 dex/kpc to −0.06 dex/kpc during the last 9 Gyr, or from −0.08 dex/kpc to −0.06 dex/kpc during the last 5 Gyr.

Key words. Galaxy: abundances – Galaxy: evolution – planetary nebulae: general

1. Introduction

Radial abundance gradients in the Galaxy have been determined by a variety of objects, including HII regions, planetary nebulae (PN), B stars, open clusters and cepheids (Henry & Worthey 1999; Maciel 2000; Rolleston et al. 2000). Several elements have been investigated, especially oxygen, sulphur, neon and argon in photoionized nebulae (Maciel & Quireza 1999; Deharveng et al. 2000) and iron in open cluster stars and cepheids (Friel 1999; Andrievsky et al. 2002a, 2002b). In the case of the O/H ratio, recent determinations from HII regions, PN and B stars point to an average gradient in the range −0.04 to −0.07 dex/kpc, taking into account an average uncertainty of 0.02 dex/kpc for most determinations.

Abundance gradients play a distinctive role as a constraint to chemical evolution models. In fact, several recently computed models, based on widely differing assumptions, point to the radial gradients as one of the most important constraints, especially when one takes into account not only their magnitudes, but also their space and time variations (see for example Hou et al. 2000; Chiappini et al. 2001; and Alibés et al. 2001).

Planetary nebulae are particularly useful in the study of the gradients and their variations (Peimbert 1990; Maciel & Köppen 1994; Maciel 1997, 2000; Peimbert & Carigi 1998; Maciel & Quireza 1999; Maciel & Costa 2002). They usually have bright emission spectra, so that they can be observed even at large heliocentric distances. Their derived abundances are relatively accurate, with uncertainties of about 0.1 to 0.2 dex, especially regarding the elements that are not synthesized by their progenitor stars, such as neon, argon and to some extent oxygen. On the other hand, as the offspring of intermediate mass stars, with main sequence masses roughly in the interval $1 < M/M_{\odot} < 8$, they are representative of objects spanning a relatively large age interval, so that it is expected that groups of PN of different ages may display different abundance variations, thus reflecting the time evolution of the gradients. The PN distances are a possible source of error, as they are not as well determined as in the case of B stars or HII regions, for example. However, it has been shown that the use of different distance scales, both individual and statistical, apparently compensates for this uncertainty (see for example Maciel & Köppen 1994). Moreover, it should be recalled that in order to determine the PN gradients larger samples are generally used as compared with HII regions.

In this paper, we present an estimate of the time variation of the O/H radial abundance gradient based on a large sample of galactic PN with relatively accurate abundances and distances. From the observed oxygen abundances, we determine the [Fe/H] metallicity using a correlation based on disk stars, and the progenitor ages are obtained through an age-metallicity

Send offprint requests to: W. J. Maciel,
e-mail: maciel@astro.iag.usp.br

relation. In Sect. 2 we describe our sample, in Sect. 3 we discuss the [O/H] × [Fe/H] relation for disk stars. The ages of the objects are estimated in Sect. 4, and we present our method to determine the abundance gradients as a function of age. Finally, Sect. 5 presents our results and discussion.

2. The data

The sample includes about 240 nebulae, most of which have oxygen abundances by number log (O/H) and distances from the samples of Maciel & Quireza (1999) and Maciel & Köppen (1994), to which the reader is referred for details on the abundances and references. About 40 new nebulae have been included, basically from recent observations from our own group, secured at the 1.52 m ESO telescope at La Silla and the 1.60 m LNA telescope in Brazil (Costa et al. 1996, 1997, 2002). Most of the new objects belong to a project to derive accurate and homogeneous abundances of PN located near the anticentre direction. A detailed analysis of the new observational data, plasma diagnostics and abundances, as well as a study of the space variations of the abundance gradients along the galactic disk is given elsewhere (Costa et al. 2002). It should be mentioned that most O/H abundance determinations are based on the so-called "empirical" method, according to which the total abundances are obtained from ionic abundances with the use of ionization correction factors for the unseen species. The ionic abundances depend on the plasma diagnostic parameters, namely the electron temperature and density, which are derived from selected line ratios (see for example Peimbert 1990 and references therein). This procedure implies average uncertainties of about 0.1 to 0.2 dex for the abundances of most elements and up to 0.02 dex/kpc for the derived gradients. These uncertainties are able to accomodate any systematic variations with the galactocentric distance (see for example Martins & Viegas 2000). In fact, the presence of abundance gradients can also be detected by considering abundances derived by other methods, such as photoionization models or detailed individual analysis, and the main discussions refer to the magnitude of the gradients.

Our sample consists only of disk nebulae, so that PN of Types IV (halo objects) according to the Peimbert (1978) classification system, or of Type V (bulge objects, see Maciel 1989) are not included. Most of the objects are classified as Type II (disk objects, intermediate mass progenitors), but PN of Type I (disk objects, large mass progenitors) and III (thick disk objects, showing large deviations from the galactic rotation curve) are also included, so that the average dispersion of the oxygen abundances of the whole sample is expected to be larger than in Maciel & Quireza (1999).

There are some suggestions that Type I PN may show some effects of ON cycling in their oxygen abundances, but current evidences are not conclusive (Peimbert & Carigi 1998; Torres-Peimbert & Peimbert 1997). Furthermore, the amount of oxygen depletion from this process is expected to be much lower than the average abundance dispersion and restricted to the objects of larger masses, which make up a small fraction of the sample.

3. The [O/H] × [Fe/H] relation

The determination of the radial O/H abundance gradient was performed in a similar way as in Maciel & Köppen (1994), and simple linear fits have been obtained. The O/H abundances by number of atoms have been converted into the usual [O/H] abundances relative to the Sun using the solar oxygen abundance $\log (O/H)_{\odot} + 12 = 8.83$ (Grevesse & Sauval 1998), so that we have the relation

$$[O/H] = \log (O/H) - \log (O/H)_{\odot}. \quad (1)$$

Iron abundances are very difficult to determine from PN and their central stars, basically because the iron lines are very weak in PN spectra, and a presumably large fraction of iron is condensed in grains (see for example Perinotto et al. 1999 and Deetjen et al. 1999). In order to convert from [O/H] to the iron metallicities [Fe/H], we have used the extensive sample of disk stars by Edvardsson et al. (1993), from which we derive the relationship

$$[Fe/H] = 0.0317 + 1.4168\,[O/H], \quad (2)$$

valid approximately in the range $-1.0 < [Fe/H] < 0.5$. The average uncertainty of the [Fe/H] metallicity is roughly 0.1 dex. For this relation we have determined an average uncertainty for the slope of 0.0488, and for the intercept the uncertainty is 0.0158. The correlation coefficient is $r = 0.9536$, which reflects the good fit of Eq. (2), as can be seen in Fig. 1.

In order to test the applicability of Eq. (2) to the galactic disk as well as to the solar neighbourhood, we have made some comparison with the [Fe/H] × [O/H] relation as obtained for different sets of galactic objects by different authors. A convenient set has been recently analysed by Maciel (2002), in a study of the use of radial abundance gradients mainly derived from young objects in the determination of the [O/Fe]×[Fe/H] relation in the galactic disk. The main results are shown in Fig. 2. In this figure, the solid line shows the relation given by Eq. (2). The dotted curve shows results of theoretical models by Matteucci et al. (1999), which follow models by Chiappini et al. (1997), and are representative of models predicting a [O/Fe] plateau for metallicities under solar, without a significant increase in the [O/Fe] ratio above 0.5 dex for $[Fe/H] \leq -2$. The dashed line is the predicted relationship on the basis of the radial gradients of young objects in the galactic disk, at galactocentric distances $4 \leq R(\mathrm{kpc}) \leq 12$, as discussed by Maciel (2002). The figure also includes some representative observational data by Barbuy & Erdelyi-Mendes (1989), asterisks; Boesgaard et al. (1999), filled squares; Edvardsson et al. (1993), crosses; Israelian et al. (1998), solid dots; Spiesman & Wallerstein (1991), open circles; Spite & Spite (1991), plus signs; Takeda et al. (2002), empty squares; Mishenina et al. (2000), open stars, and Cavallo et al. (1997), filled stars, as recomputed by Mishenina et al. (2000).

It can be seen from Fig. 2 that the observational data and models show a reasonable agreement, especially for metallicities close to and slightly lower than the solar value. For the lowest metallicities the spread is somewhat larger and the points lie, on the average, under the line corresponding to Eq. (2), but the relatively sparse data are still reasonably well represented

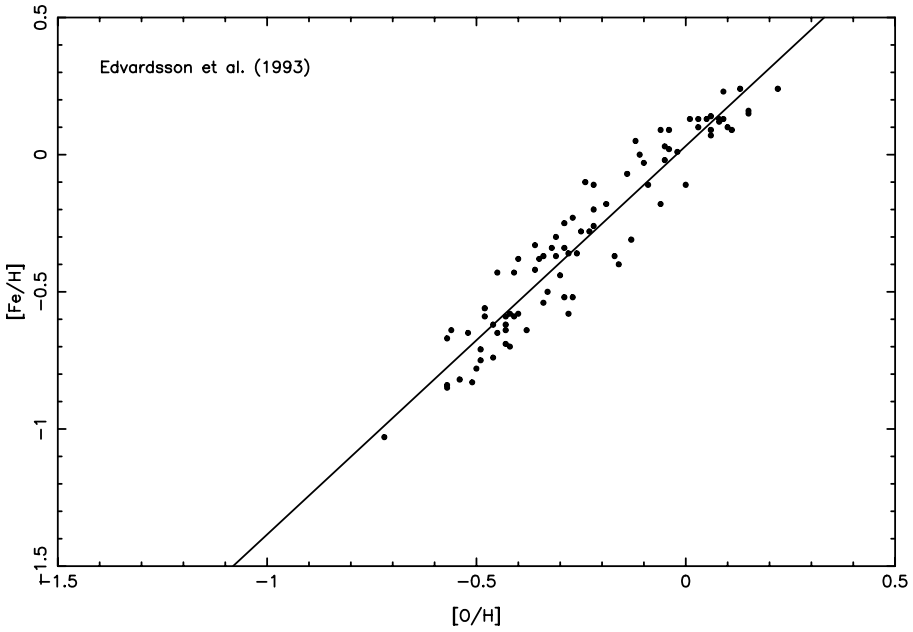

Fig. 1. Correlation between [Fe/H] and [O/H] obtained from the data of Edvardsson et al. (1993).

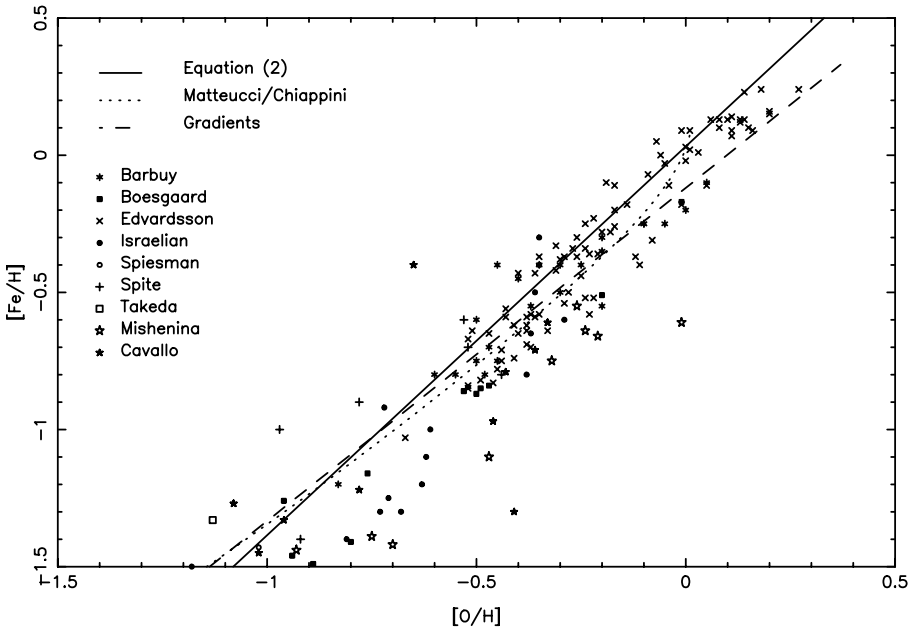

Fig. 2. A comparison of the average relation given by Eq. (2) (solid line), theoretical models by Matteucci et al. (1999, dotted line), the predicted relation derived from the gradients of young objects (Maciel 2002, dashed line) and selected observational data from a number of sources (see text).

by the solid line. Part of the scatter in Fig. 2 may be due to the use of different scales of stellar parameters such as effective temperatures, gravities and metallicities, to the adoption of different atomic parameters or the neglecting of NLTE effects. The relation given by the theoretical models (dotted line) is representative of the galactic disk, since the calculated variations of the [O/Fe] × [Fe/H] relation from galactocentric distances $R = 4$ kpc to $R = 14$ kpc are expected to be small (Matteucci 1996). The gradient derived line (dashed line) was based on O/H and [Fe/H] gradients for young objects (HII regions, hot stars and open clusters) located at galactocentric radii roughly in the range $R = 4$ kpc to $R = 16$ kpc. On the other hand, the stellar data include objects in the thin disk, thick disk and even some metal-poor halo stars. Therefore, it can be concluded that Eq. (2) represents fairly well the average [Fe/H] × [O/H] relation in the disk, so that any galactocentric variation of this relation is absorbed by the expected scatter, as shown in Fig. 2.

4. The [Fe/H] × τ relation

The main difficulty in the estimate of the time variation of the abundance gradients from planetary nebulae lies in the

determination of reliable ages for the central stars. One possibility is to use an average age-metallicity relation, since chemical abundances from PN are relatively well determined, and several age-metallicity relations derived recently are similar, albeit with a considerable scatter (see Rocha-Pinto et al. 2000 for a recent discussion). In fact, there has been some discussion on the existence of such a relationship (Feltzing et al. 2001), but a critical analysis of the available data suggests some increase in the average metallicities with time, which is expected on the basis of the current ideas on the chemical evolution of the Galaxy.

Age-metallicity relationships have been determined by a number of people (Twarog 1980; Carlberg et al. 1985; Meusinger et al. 1991; Edvardsson et al. 1993; Rocha-Pinto & Maciel 1998; Rocha-Pinto et al. 2000), based on a variety of samples and techniques. In general, these relationships are similar, which is particularly true for the relations derived by Edvardsson et al. (1993) and the recent results based on chromospheric ages by Rocha-Pinto et al. (2000). This can be seen from Fig. 14 of Rocha-Pinto et al. (2000), where the new relation is compared with the relation by Edvardsson et al. (1993) adopting 1 Gyr average bins, as well as with the results by Twarog (1980), Carlberg et al. (1985) and Meusinger et al. (1991). These results apply strictly to the solar neighbourhood, since most of the stars included in the samples are nearby objects with HIPPARCOS parallaxes. However, the observed scatter in these relationships is considerably large, amounting up to 0.26 dex for the results of Edvardsson et al. (1993) and about 0.13 dex for the relation obtained by Rocha-Pinto et al. (2000), so that it probably includes any differences in the corresponding relationships at different galactocentric distances. This can be seen, for example, in Fig. 14a of Edvardsson et al. (1993), where the metallicity [Fe/H] is plotted against age using different symbols for stars at galactocentric distances $R < 7$ kpc, $7 < R$(kpc) < 9 and $R > 9$ kpc, spanning radii from 4 kpc to 11 kpc (see also Table 14 of Edvardsson et al. 1993). Even though the sample at $7 < R$(kpc) < 9 is the most complete statistically, it can be seen that all objects can be reasonably fit in the average age-metallicity relation, in view of the large scatter.

In order to take into account any difference in the age-metallicity relationship introduced by differente galactocentric distances, Edvardsson et al. (1993) went a step further and derived an average age-metallicity-radius relation given by

$$\log \tau = 0.872 - 0.303\ [\mathrm{Fe/H}] - 0.038\ R, \qquad (3)$$

where τ is the stellar age in Gyr and R is the galactocentric distance in kpc (see Eq. (19) of Edvardsson et al. 1993), with a typical uncertainty of $\sigma(\log \tau) \simeq 0.10$. This equation was based on stars with $\log \tau < 1.0$, a condition fulfilled by all objects in our sample, the majority of which have $\tau \simeq 5$ Gyr, or $\log \tau \simeq 0.70$.

We can compare the ages derived by Eq. (3) with the actual average age-metallicity relation by Edvardsson et al. (1993) for different galactocentric distances as given in Table 14 of that paper. We performed this calculation for the galactocentric radii $4 < R$(kpc) < 11, and Fig. 3 shows representative examples for $6 < R$(kpc) < 7 and $10 < R$(kpc) < 11. The histogram data are from Table 14 of Edvardsson et al. (1993) while the dashed lines are results from the application of Eq. (3), adopting $R = 6.5$ kpc and $R = 10.5$ kpc, respectively. It can be seen that the dashed lines produce similar results as the age-metallicity relation, considering that our objects have ages $\log \tau < 1$ Gyr, peaking at $\tau \simeq 0.7$ Gyr, as already mentioned. Therefore, the use of Eq. (3) introduces a correction to the age-metallicity relation for the solar neighbourhood adjusting it to other galactocentric distances in the range of 4 to 11 kpc approximately. Of course, the uncertainties in the derived ages are still considerably large, irrespective of the galactocentric radius, as can be seen by the scatter in the age-metallicity relations quoted here. However, in this study we are mainly interested in the time *variation* of the gradients, so that, in fact, only *relative* ages will be important in our analysis. Finally, as a further check of our results, in Sect. 5.2. we will discuss a totally independent way of estimating the ages of the PN central stars and its effect on the time variation of the O/H abundance gradient.

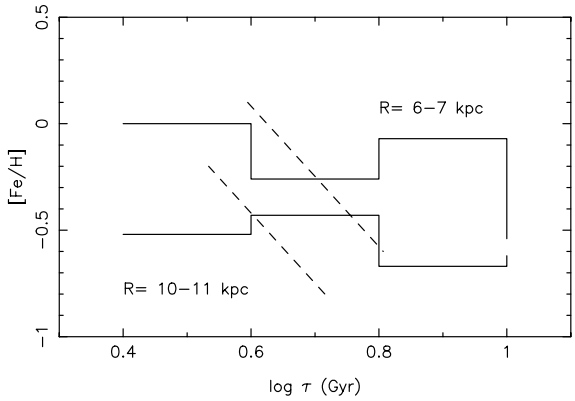

Fig. 3. A comparison of age-metallicity relation as derived by Edvardsson et al. (1993) for stars in the galactocentric ranges $6 < R$(kpc) < 7 (top histogram) and $10 < R$(kpc) < 11 (bottom histogram) with the estimated relation calculated by Eq. (3) (dashed lines), where we have used $R = 6.5$ kpc and $R = 10.5$ kpc, respectively.

5. Results and discussion

5.1. Time variation of the O/H gradient

The PN sample has been divided into three groups of increasing ages, namely Groups I, II, and III. Since all objects have ages under 10 Gyr, we have considered initially the following groups, which we will call Case A: Group I: $0 < \tau$(Gyr) < 3, Group II: $3 < \tau$(Gyr) < 6, and Group III: $\tau > 6$ Gyr.

The derived gradients are shown in Fig. 4, where we have taken $R_0 = 8$ kpc for the galactocentric distance of the LSR, in agreement with the value adopted by Edvardsson et al. (1993). In fact, the main results of this paper are unchanged if we adopt different values such as the IAU recommended value $R_0 = 8.5$ kpc, or some recently determined result such as $R_0 = 7.6$ kpc (see for example Maciel & Quireza 1999). The figure shows the separation of Group I (squares), II (dots) and III (crosses), and the linear gradients of each group (dex/kpc).

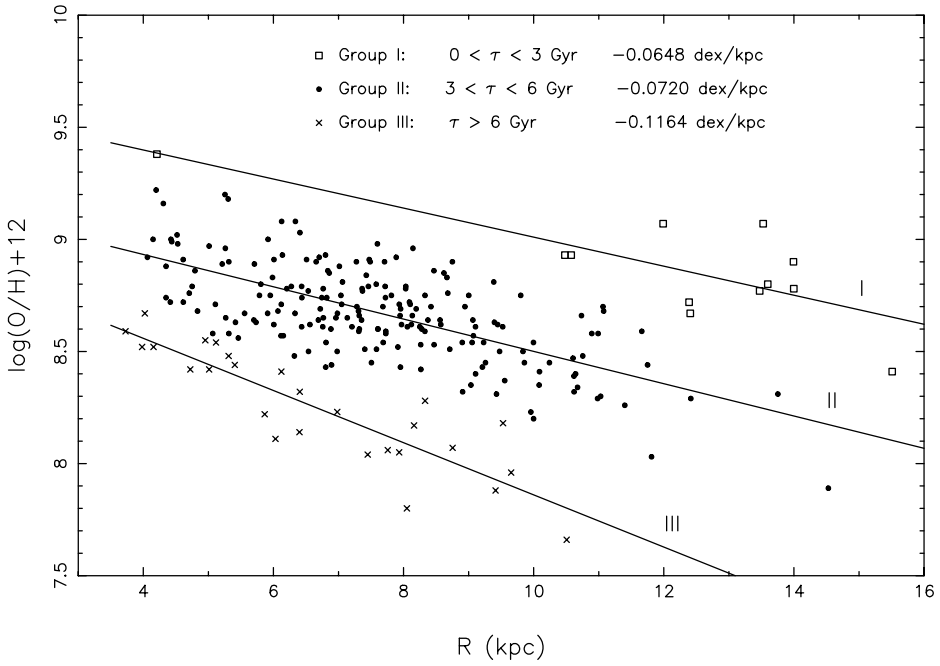

Fig. 4. Radial O/H gradients from PN of Group I (squares), Group II (dots) and Group III (crosses) for Case A.

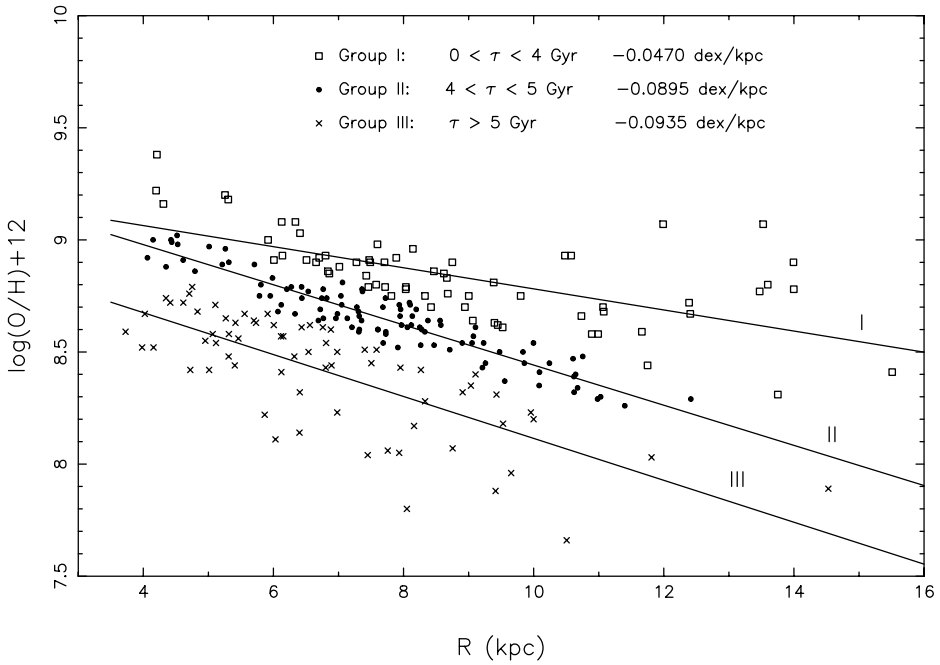

Fig. 5. The same as Fig. 4 for Case B.

The values of the gradients (dex/kpc), the associated uncertainties σ_g, the correlation coefficients r and the number of objects in each class are given in Table 1. We can see that Group I is underpopulated compared to the remaining groups, reflecting the lack of the most massive and presumably younger objects, which affects the derived slope. Therefore, we have alternatively defined Case B as follows: Group I: $0 < \tau(\mathrm{Gyr}) < 4$; Group II: $4 < \tau(\mathrm{Gyr}) < 5$, and Group III: $\tau > 5$ Gyr, so that we have approximately the same number of nebulae in each age group. The corresponding results are shown in Fig. 5 and also in Table 1.

From the figures and the uncertainties in the slopes given in Table 1, it can be seen that there is a clear tendency for the O/H gradient to flatten out with time. This tendency is clear in both Cases A and B, and is particularly strong between Groups III and II (Case A) and Groups II and I (Case B). This is confirmed by the inspection of the uncertainties in the slopes as given in Table 1. For Case A, the gradients have flattened from −0.11 dex/kpc to −0.06 dex/kpc, while for Case B, we have −0.09 dex/kpc for the oldest group and −0.05 dex/kpc for the youngest one. Overall, one could conclude that the gradients flattened out from −0.11 dex/kpc to −0.06 dex/kpc in about

Table 1. Results of the linear fits.

Case A	I	II	III
$\frac{d\log(O/H)}{dR}$	−0.0648	−0.0720	−0.1164
σ_g	0.0168	0.0057	0.0127
r	−0.77	−0.67	−0.88
n	12	195	27
Case B	**I**	**II**	**III**
$\frac{d\log(O/H)}{dR}$	−0.0470	−0.0895	−0.0935
σ_g	0.0070	0.0034	0.0102
r	−0.64	−0.94	−0.75
n	66	99	69

9 Gyr, or from −0.08 dex/kpc to −0.06 dex/kpc in the last 5 Gyr only.

5.2. Ages of the central stars from their main sequence masses

In view of the uncertainties involved in the estimate of the ages of the stars in our sample, which are basically due to the the adopted age-metallicity relationship, it is interesting to evaluate the time variation of the abundance gradients based on independent age estimates. This can be achieved on the basis of a correlation between the N/O abundances and the central star masses recently discussed by Cazetta & Maciel (2000), which is supported by recent theoretical calculations (see for example Marigo 2000). According to this relation, if N/O is the nitrogen abundance relative to oxygen by number of atoms, the core mass M_c in solar masses is given by the relations

$$M_c \simeq 0.7242 + 0.1742\ \log(N/O) \quad (4)$$

for $\log(N/O) \leq -0.26$ and

$$M_c \simeq 0.825 + 0.936\ \log(N/O) + 1.439\ [\log(N/O)]^2 \quad (5)$$

for $\log(N/O) > -0.26$. These relationships are valid in the approximate range $-1 < \log(N/O) < 0.2$. The main sequence mass M_{ms} can be obtained through a initial mass-final mass relation given by

$$M_c \simeq 0.5 + 0.1\ M_{ms}. \quad (6)$$

This set of equations characterizes the so-called *low-mass calibration* (see a detailed discussion in Cazetta & Maciel 2000 and Maciel 2001), and shows a better agreement with the recent discussions on the PN central star masses by Stasińska et al. (1997), Zhang (1993), with the mass-N/O abundance relation by Marigo et al. (1996) and the initial mass-final mass relations by Groenewegen & de Jong (1993) and Blöcker & Schönberner (1990).

From Eqs. (4)–(6) above the main sequence mass can be estimated from the N/O abundances. The stellar age can then be derived using the average lifetimes based on stellar evolutionary models for Population I stars given by Bahcall & Piran (1983), that is

$$\log t(M_{ms}) = 10.0 - 3.6\ \log M_{ms} + (\log M_{ms})^2 \quad (7)$$

where $t(M_{ms})$ is given in years and M_{ms} again in solar masses. This relation has an estimated uncertainty of about 10% according to Bahcall & Piran (1983) or somewhat larger according to Scalo (1986), but in any case it is expected to produce reliable *relative* ages.

We have applied the procedure described above to the PN central stars in our sample, using revised N/O abundances listed by Cazetta & Maciel (2000) and Maciel & Chiappini (1994). Again dividing the objects into Groups I, II and III, we obtained the results shown in Fig. 6, where the symbols have the same meaning as in Fig. 4. The slopes are given in the figure, and the corresponding uncertainties and correlation coefficients are in the range $\sigma_g \simeq 0.013$ to 0.021 and $|r| \simeq 0.67$ to 0.88. Although the available sample is smaller than in the case of the previous figures, and some superposition can be observed in the different classes, it is clear that the same pattern is observed here, that is, the youngest objects display flatter gradients, as can be seen from the slopes given on the top of the figure. Since the adopted procedures to estimate the ages in the case of Figs. 4 and 6 are totally independent from each other, we have a further evidence that the *relative* behaviour of the gradients is indeed reflected by the results shown in Figs. 4 and 5.

5.3. Discussion

A schematic plot of the results of Sect. 5.1. is shown in Fig. 7, where the solid lines refer to Case A and B, and the dotted line is a reference line at −0.07 dex/kpc. This reference line is usually considered as an average value for the younger population, comprising HII regions and B stars, but this should be regarded with caution in view of the recent discussions on these objects as well as on open cluster stars and cepheids (see references in the Introduction). A realistic uncertainty for the slope of the young population can be roughly taken as 0.02 dex/kpc. For comparison purposes, we also include in the figure the results of the theoretical models by Hou et al. (2000) based on an inside-out scenario for the formation of the disk with metallicity dependent yields (dashed line). The agreement is remarkable, especially during the last 5 Gyr, which include most of our objects, and for which the derived ages are relatively more accurate. From these data, we can estimate an average flattening rate of 0.002 dex kpc^{-1} Gyr^{-1} (Case A) or a rate of about 0.004 dex kpc^{-1} Gyr^{-1}, considering both cases in the last 5 Gyr, suggesting that the O/H gradient has not changed more than 30% in average during the last few Gyr. At earlier times, however, our results are consistent with a steeper rate, although the corresponding uncertainties are larger.

It is interesting to compare these results with earlier estimates based on planetary nebulae. Maciel & Köppen (1994) found some evidences for a steepening of the gradients, especially those of Ne, Ar and S, while for the O/H ratio some steepening could be obtained for PN of Peimbert types II and III only. However, the average ages attributed to the different PN types were very approximate, and no effort was made to establish individual ages. These average values have also been used by Maciel & Quireza (1999), leading to the conclusion that the gradients steepen out in time at a ratio of about

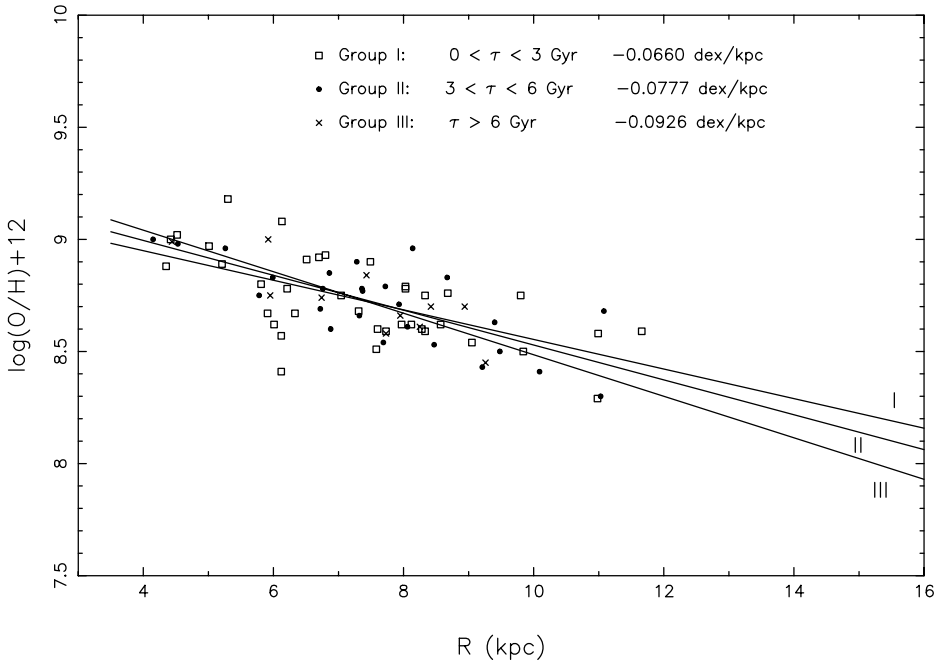

Fig. 6. Radial O/H gradients from PN of Group I (squares), Group II (dots) and Group III (crosses) for Case A. The ages of the central stars have been calculated as described in Sect. 5.2.

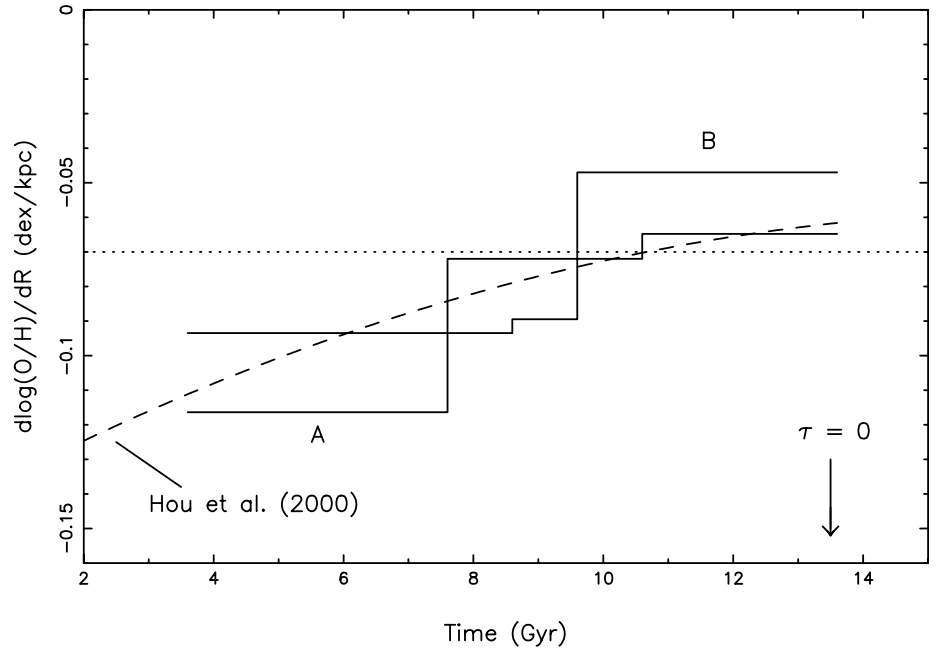

Fig. 7. Time variation of the PN gradients for Case A and B (solid lines). Also shown are results from theoretical models by Hou et al. (2000, dashed curve).

0.004 dex kpc^{-1} Gyr^{-1} in the Galaxy, a result which is not confirmed by the present paper. The main difference between the present work and these early attempts, apart from our larger and more accurate sample, refers to the definition of the age groups. Maciel & Köppen (1994) adopted literally the Peimbert classification scheme, which, strictly speaking, attributes different and increasing ages for the progenitor stars of PN of types I, II and III, respectively. In this work, we have not assumed any correlation between the PN type and the progenitor age, and made an effort to derive individual ages, so that we expect the present results to be more reliable. We notice that most Type I PN in our sample belong to age Group II, most Type II PN are spread between Groups I and II, while PN of Type III belong either to Groups II or III. Finally, most of the objects in Group III are indeed Type III PN (Case A). We can then conclude that within the disk PN of a given type there are objects with a reasonable age span. In other words, there seems to be some overlapping in the progenitor masses – and ages –

within the Peimbert types, which was not accounted for by the earlier attempts to estimate the time variation of the gradients, and probably explains the different results presented here as compared with the earlier work. In fact, as recently discussed by Peimbert & Carigi (1998), some overlapping occurs in the masses of the progenitors of PN of types II and III, which supports our present views.

Acknowledgements. This work was partially supported by CNPq and FAPESP.

References

Alibés, A., Labay, J., & Canal, R. 2001, A&A, 370, 1103
Andrievsky, S. M., Kovtyukh, V. V., Luck, R. E., et al. 2002, A&A, 381, 32
Andrievsky, S. M., Bersier, D., Kovtyukh, V. V., et al. 2002, A&A, 384, 140
Bahcall, J. N., & Piran, T. 1983, ApJ, 267, L77
Barbuy, B., & Erdelyi-Mendes, M. 1989, A&A, 214, 239
Blöcker, T., & Schönberner, D. 1990, A&A, 240, L11
Boesgaard, A. M., King, J. R., Deliyannis, C. P., & Vogt, S. S. 1999, AJ, 117, 492
Carlberg, R. G., Dawson, P. C., Hsu, T., & VandenBerg, D. A. 1985, ApJ, 294, 674
Cavallo, R. M., Pilachowski, C. A., & Rebolo, R. 1997, PASP, 109, 226
Cazetta, J. O., & Maciel, W. J. 2000, Rev. Mex. Astron. Astrofis., 36, 3
Chiappini, C., Matteucci, F., & Gratton, R. 1997, ApJ, 477, 765
Chiappini, C., Matteucci, F., & Romano, D. 2001, ApJ, 554, 1044
Costa, R. D. D., Chiappini, C., Maciel, W. J., & Freitas-Pacheco, J. A. 1996, A&AS, 116, 249
Costa, R. D. D., Chiappini, C., Maciel, W. J., & Freitas-Pacheco, J. A. 1997, in Advances in Stellar Evolution, ed. R. T. Rood, & A. Renzini (CUP, Cambridge), 159
Costa, R. D. D., Maciel, W. J., & Uchida, M. M. M. 2002, in preparation
Deetjen, J. L., Dreizler, S., Rauch, T., & Werner, K. 1999, A&A, 348, 940
Deharveng, L., Peña, M., Caplan, J., & Costero, R. 2000, MNRAS, 311, 329
Edvardsson, B., Andersen, J., Gustafsson, B., et al. 1993, A&A, 275, 101
Feltzing, S., Holmberg, J., & Hurley, J. R. 2001, A&A, 377, 911
Friel, E. D. 1999, Ap&SS, 265, 271
Grevesse, N., & Sauval, A. J. 1998, Space Sci. Rev., 85, 161
Groenewegen, M. A. T., & de Jong, T. 1993, A&A, 267, 410
Henry, R. B. C., & Worthey, G. 1999, PASP, 111, 919
Hou, J. L., Prantzos, N., & Boissier, S. 2000, A&A, 362, 921
Israelian, G., García López, R. J., & Rebolo, R. 1998, ApJ, 507, 805
Maciel, W. J. 1989, in IAU Symp. 131, ed. S. Torres-Peimbert (Kluwer, Dordrecht), 73
Maciel, W. J. 1997, in IAU Symp. 180, ed. H. J. Habing, & H. J. G. L. M. Lamers (Kluwer, Dordrecht), 397
Maciel, W. J. 2000, in The Evolution of the Milky Way, ed. F. Matteucci, & F. Giovannelli (Kluwer, Dordrecht), 81
Maciel, W. J. 2001, Ap&SS, 277, 545
Maciel, W. J. 2002, Rev. Mex. Astron. Astrofis., Ser. Conf., 12, 207
Maciel, W. J., & Chiappini, C. 1994, Ap&SS, 219, 231
Maciel, W. J., & Costa, R. D. D. 2002, in IAU Symp. 209, ed. R. Sutherland, S. Kwok, & M. Dopita, (ASP, San Francisco), in press
Maciel, W. J., & Köppen, J. 1994, A&A, 282, 436
Maciel, W. J., & Quireza, C. 1999, A&A, 345, 629
Marigo, P. 2000, in The Evolution of the Milky Way, ed. F. Matteucci, & F. Giovannelli (Kluwer, Dordrecht), 481
Marigo, P., Bressan, A., & Chiosi, C. 1996, A&A, 313, 545
Martins, L. P., & Viegas, S. M. M. 2000, A&A, 361, 1121
Matteucci, F. 1996, Fund. Cosm. Phys., 17, 283
Matteucci, F., Romano, D., & Molaro, P. 1999, A&A, 341, 458
Meusinger, H., Reimann, H.-G., & Stecklum, B. 1991, A&A, 245, 57
Mishenina, T. V., Korotin, S. A., Klochkova, V. G., & Panchuk, V. E. 2000, A&A, 353, 978
Peimbert, M. 1978, in IAU Symp. 76. ed. Y. Terzian (Reidel, Dordrecht), 215
Peimbert, M. 1990, Rep. Prog. Phys., 53, 1559
Peimbert, M., & Carigi, L. 1998, in ASP Conf. Ser. 147, ed. D. Friedli, M. G. Edmunds, C. Robert, & L. Drissen, 88
Perinotto, M., Bencini, C. G., Pasquali, A., et al. 1999, A&A, 347, 967
Rocha-Pinto, H. J., & Maciel, W. J. 1998, MNRAS, 298, 332
Rocha-Pinto, H. J., Maciel, W. J., Scalo, J., & Flynn, C. 2000, A&A, 358, 850
Rolleston, W. R. J., Smartt, S. J., Dufton, P. L., & Ryans, R. S. I. 2000, A&A, 353, 537
Scalo, J. M. 1986, Fund. Cosm. Phys. 11, 1
Spiesman, W. J., & Wallerstein, G. 1991, AJ, 102, 1790
Spite, M., & Spite, F. 1991, A&A, 252, 689
Stasińska, G., Gorny, S. K. & Tylenda, R. 1997, A&A, 327, 736
Takeda, Y., Takada-Hidai, M., Sato, S., et al. 2002, ApJ, in press [astro-ph/0007007]
Torres-Peimbert, S., & Peimbert, M. 1997, in IAU Symp. 180, ed. H. J. Habing, & H. J. G. L. M. Lamers (Kluwer, Dordrecht), 175
Twarog, B. A. 1980, ApJ, 242, 242
Zhang, C. Y. 1993, ApJ, 410, 239